CHEMISTRY LETTERS, pp. 1325-1328, 1989.

Structure and Bonding of Two Modifications of $CsSnI_3$ by Means of Powder X-Ray Diffraction, ^{127}I NQR, and DTA

Koji YAMADA, Tomoko TSURITANI, Tsutomu OKUDA, and Sumio ICHIBA
Department of Chemistry, Faculty of Science, Hiroshima University,
Higashisenda-machi, Naka-ku, Hiroshima 730

A first-order phase transition accompanied by a color change from green to black was observed for $CsSnI_3$ at about 425 K. These two modifications showed quite different ^{127}I NQR spectra suggesting drastic structural change. High temperature modification has a perovskite structure with semi-metallic electric conductivity. The anion structure and bonding for the two modifications have been discussed on the basis of ^{127}I NQR and X-ray diffraction data.

Trihalogenostannate(II) anion, SnX_3^-, provides us still interesting problems concerning the structure and bonding because of the typical hypervalent character of the Sn(II) electronic configuration. According to X-ray structure analysis concerning the SnX_3^- anion, the nearest neighbors around the tin environment are regular or distorted octahedral sharing bridging halogens. In our previous paper four models were proposed depending upon the distortion of the octahedral environment as shown in Fig. 1.[1,2] In the octahedral environment, each trans X-Sn-X or X-Sn$\cdots$X bond could be described as a three-center-four-electron (3c-4e) bond mainly using 5p orbitals of the central Sn atom. Hence the two X-Sn bonds in the linear X-Sn-X arrangement affect each other such that if one Sn-X bond becomes stronger the other bond at the trans position weaker. This behavior is essentially similar to that found in the linear I_3^- anion which is symmetric ($(C_6H_5)_4AsI_3$; I-I=2.90Å) or asymmetric (NH_4I_3; I-I=2.79 and 3.11Å).[3,4] Several different types of phase-transitions accompanied by structural changes of the SnX_3^- anion have been reported for $CsSnCl_3$,[5,6] $KSnBr_3.H_2O$[1] and $CH_3NH_3SnBr_3$.[2] In this paper structural phase-transitions of $MSnI_3$ (M=Cs and CH_3NH_3) were reported and the anion structural change was discussed on the basis of ^{127}I NQR and powder X-ray diffraction. Two modifications of $CsSnI_3$ have been reported by Scaife,[6] but neither complete ^{127}I NQR nor dc conductivity has been observed so far.

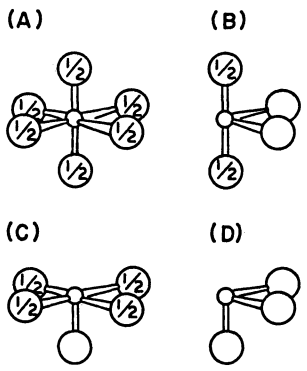

Fig. 1. Four models of SnX_3^-.

High-temperature form of $CsSnI_3$ was obtained as a single crystal in a silica tube using a equimolar mixture of SnI_2 and CsI by means of a Bridgman

technique. Low-temperature form was obtained grinding the single crystal using agate mortar. $CH_3NH_3SnI_3$ was obtained as black crystals by a solid state reaction between SnI_2 and CH_3NH_3I at 200 °C for several days. Powder X-ray diffraction was measured at room temperature by means of a Rigaku Rad-B system using Cu K_α radiation. ^{127}I NQR spectra were detected using a pulsed spectrometer (Matec model 5100+525). Because of the large NQR line width, no free-induction decay signal could be detected but strong echo signals were observed at 77 K. In the case of the high temperature modification of $CsSnI_3$, a well-powdered sample or mixture with Al_2O_3 powder was used, since the electric conductivity of the sample reduced the sensitivity of the NQR. DTA measurements were performed with a home-made apparatus consisted of a copper block and Cu-constantan thermocouples, using a sample sealed in a glass tube in order to avoid the decomposition or oxidation at high temperature. Dc conductivity was measured employing a 4-probe method using a single crystal for $CsSnI_3$ and a pellet sample for $CH_3NH_3SnI_3$.

Powder X-ray diffraction, DTA, and dc-conductivity. Figure 2(A) shows the powder X-ray diffraction pattern for $CsSnI_3$(G) (hereafter abbreviations (G) and (B) are used for low and high temperature modifications, respectively, due to their characteristic colors, green and black). The powder pattern for $CsSnI_3$(G) agreed very well with that calculated from the structural parameters reported by Mauersberger and Huber.[7] In this orthorhombic modification, $CsSnI_3$(G), the tin environment is distorted considerably from a regular octahedron and the anion is regarded as a square pyramid having model (C).(Fig. 4(A))[7] The DTA curve for this sample (Fig. 3) showed a strong endothermic peak (a) at 425 K accompanying a color change from green to black. In the DTA sample tube this high temperature phase remained black down to 77 K, so that the peak (b) or the base line shift at (c) was not due to a phase transition from $CsSnI_3$(B) to $CsSnI_3$(G). On

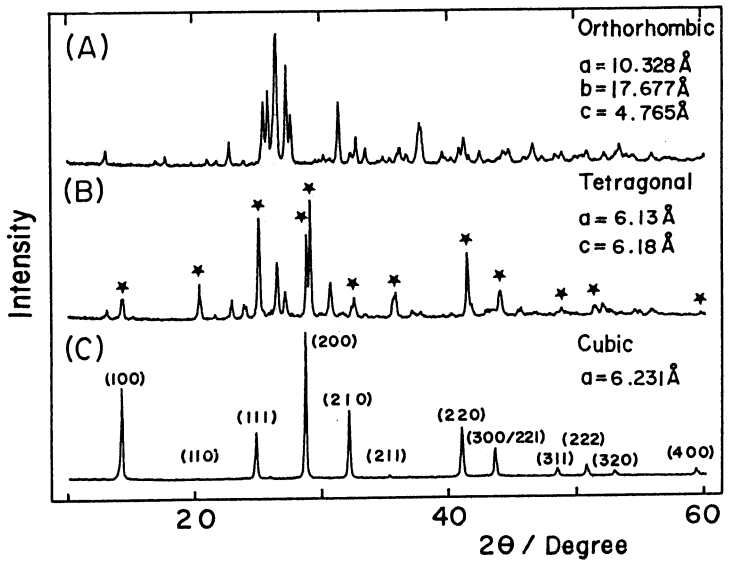

Fig. 2. X-Ray powder patters. A:$CsSnI_3$(G), B:$CsSnI_3$(B), C:$CH_3NH_3SnI_3$.

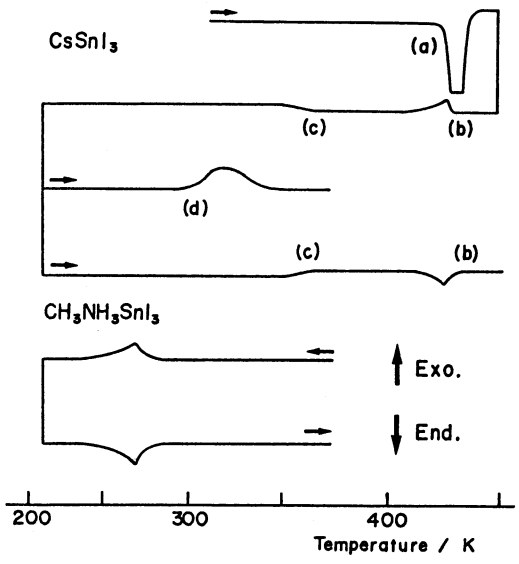

Fig. 3. DTA curves for $MSnI_3$(M=Cs and CH_3NH_3). Heating or cooling rate=2°C/min.

Table 1. ^{127}I NQR parameters for two modifications of $CsSnI_3$ at 77 and 293 K[a)]

Compound	ν_1/MHz	ν_2/MHz	e^2Qqh^{-1}/MHz	η	Assignment[b)]
$CsSnI_3$(B)	88.6 (88.2)	-	591.	0[c)]	
	94.2 (90.5)	-	628.	0[c)]	
$CsSnI_3$(G)	25.30	43.1	147.5	0.376	I(3)
	58.25(56.86)	99.50(97.42)	340.4(333.1)	0.373(0.369)	I(2)
	81.29(79.59)	138.70(137.64)	474.5(469.8)	0.374(0.356)	I(1)

a) Parameters in parentheses correspond to 293 K.
b) Assignment on the basis of the structure shown in Fig. 2(a).
c) η =0 assumed because of the linear Sn-I-Sn bond.

heating $CsSnI_3$(B) from 200 K, on the other hand, an exothermic peak (d) corresponding to a phase transition from $CsSnI_3$(B) to $CsSnI_3$(G) was observed or, in certain cases, $CsSnI_3$(B) remained stable throughout this cycle. Figure 2(B) shows the x-ray powder pattern for the black phase observed at room temperature. The asterisks mean new reflections which are assigned to a tetragonal perovskite of $CsSnI_3$(G). These new reflections could be easily indexed referring to those of $CH_3NH_3SnI_3$, which has a typical cubic perovskite as shown in Fig. 2(C).[8)] A slight splitting at (200) and (210) reflections in $CsSnI_3$(B) suggest a slight tetragonal distortion of the perovskite. The perovskite phase was unstable especially with a mechanical shock at around room temperature, so that the diffraction pattern was a mixture with a slight extent of $CsSnI_3$(G). The dc conductivity measurement using single crystal of $CsSnI_3$(B) showed that the crystal has semi-metallic conductivity (σ =800 $\Omega^{-1}cm^{-1}$ at 77 K) with negative temperature coefficient ($d\sigma/dT<0$) in the temperature range from 77 to 400 K. At the beginning of these measurements the sample was heated above 430 K in order to get pure $CsSnI_3$(B) phase. Otherwise the conductivity decreased several orders due to the formation of $CsSnI_3$(G) phase at the surface. Cubic $CH_3NH_3SnI_3$ was also semi-metallic and showed a phase-transition at 273 K. However, there was no anomalous behavior in the dc conductivity at T_{tr}.

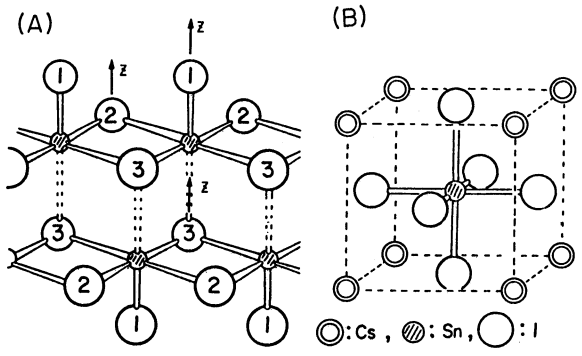

Fig. 4. Structures of SnI_3^- in $CsSnI_3$(G) and $CsSnI_3$(B).

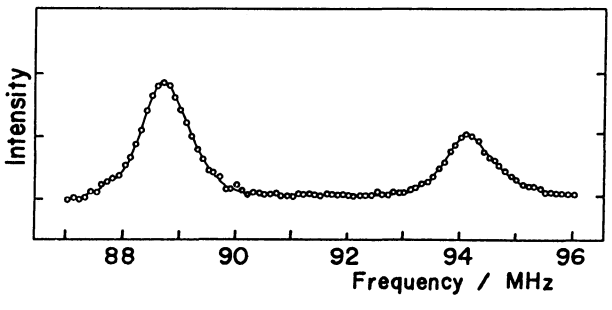

Fig. 5. ^{127}I NQR spectra for $CsSnI_3$(B) at 77 K.

^{127}I NQR for $CsSnI_3$(G) and $CsSnI_3$(B). Table 1 shows the ^{127}I NQR parameters for two modifications of $CsSnI_3$. According to the crystal structure for $CsSnI_3$(G) there are three iodine sites (i.e., terminal, bridge, and triply bridge iodines). As expected from the structure, three pair of lines ν_1(1/2 $\leftrightarrow$3/2) and ν_2(3/2$\leftrightarrow$5/2) were detected at quite different frequency regions. On the other hand, as Fig. 5 shows, $CsSnI_3$(B) showed two ^{127}I NQR lines with extremely large line width in the frequency range from 88 to 96 MHz. Both these signals belong to ν_1 transition because no signal was detected between 44 and 88 MHz due to the relation, $\nu_1 \geq \nu_2 * 0.5$. Two NQR ν_1 transitions with intensity ratio 2:1 from the lowest are consistent with the tetragonal perovskite structure, i.e., one I-Sn-I bond (6.18Å) is longer than the remaining two I-Sn-I bonds (6.13Å). The interpretation of the iodine NQR parameters is relatively simple, because the main contribution to e^2Qq_{obs}/h is the imbalance of the valence 5p orbitals, that is,

$$e^2Qq_{obs}/h = e^2Qq_p/h \cdot \left| N_z - (N_y + N_x) \right| / 2 \quad ,$$

where e^2Qq_p/h (=1192MHz) is the quadrupole coupling constant for one 5p electron and where N_i (i=x, y and z) is the population of each $5p_i$ orbital in which z axis is chosen as shown in Fig. 4. Therefore, the large differences in the observed NQR parameters can be qualitatively understandable as follows. For the iodine in $CsSnI_3$(B) and I(1) in $CsSnI_3$(G), only p_z is used for the bonding with Sn, so that a relatively large e^2Qq/h value is expected because $N_z < N_y = N_x = 2$. On the other hand in the case of triply bridging I(3), all three p orbitals take part in the bonding. Hence, a small e^2Qq/h value is expected because $2 > N_z \approx N_x = N_y$. The bridging iodine, I(2), is similar to I(3) except $N_z = 2$, so that its e^2Qq/h is expected to be larger than that of I(3). A similar bonding scheme of iodine like $CsSnI_3$(G) was found in TeI_4, in which the ^{127}I NQR ν_1 transitions were observed in the frequency range from 8 to 250 MHz.[11]

References

1) K. Yamada, T. Hayashi, T. Umehara, T. Okuda, and S. Ichiba, Bull. Chem. Soc. Jpn., 60, 4203 (1987).
2) K. Yamada, S. Nose, T. Umehara, T. Okuda, and S. Ichiba, Bull. Chem. Soc. Jpn., 61, 4265 (1988).
3) R. C. L. Mooney Stater, Acta Crystallogr., 12, 187 (1959).
4) G. Migchelsen and A. J. T. Finney, Acta Crystallogr., Sect. B, 26, 904 (1970).
5) J. Barrett, S. R. A. Bird, J. D. Donaldson, and J. Silver, J. Chem. Soc., A, 1971, 3105.
6) D. E. Scaife, P. F. Weller, and W. G. Fisher, J. Solid State Chem., 9, 308 (1974).
7) P. Mauersberger and F. Huber, Acta Crystallogr., Sect. B, 36, 683 (1980).
8) D. Weber, Z. Naturforsch., B, 33, 1443(1978).
9) J. D. Donaldson and J. Silver, J. Chem. Soc., Dalton Trans., 1973, 666.
10) D. E. Parry, M. J. Tricker, and J. D. Donaldson, J. Solid State Chem., 28, 401 (1979).
11) T. Okuda, K. Yamada, and H. Negita, Bull. Chem. Soc. Jpn., 53, 2659 (1980).

(Received March 13, 1989)